

RESEARCH

Open Access



# Linking soil organic carbon mineralization to soil physicochemical properties and bacterial alpha diversity at different depths following land use changes

Jing Guo<sup>1</sup>, Wulai Xiong<sup>1</sup>, Jian Qiu<sup>1</sup> and Guibin Wang<sup>1\*</sup>

## Abstract

**Background** Anthropogenic land use changes (LUCs) impart intensifying impacts on soil organic carbon (SOC) turnover, leading to uncertainty concerning SOC mineralization patterns and determining whether soils act as “source” or “sink” in the global carbon budget. Therefore, understanding the SOC mineralization characteristics of different LUC patterns and their potential influencing factors is crucial. An indoor incubation experiment was conducted to study the SOC mineralization patterns and their relevance to soil physicochemical properties, soil enzyme activity, SOC fractions, and bacterial alpha diversity. The soils were collected from two layers of five typical LUC patterns in Yellow Sea Forest Park, including four that were converted from wheat–corn rotation systems [a ginkgo plantation (G), a metasequoia plantation (M), a ginkgo–wheat–corn agroforestry system (GW), and a ginkgo–metasequoia system (GM)] and a traditional wheat–corn system (W).

**Results** LUCs had significant and diverse impacts on the SOC content and SOC fraction contents and on soil enzyme activity. The cumulative SOC mineralization was significantly higher in the M system than in the W and GW systems at 0–20 cm depth and higher in the G system than in the GW system at 20–40 cm depth after 60-day incubation. The mineralization ratio was highest in the W system and lowest in the GW system. The soil pH and bulk density had a significant negative correlation with the cumulative SOC mineralization, while the soil bacterial Shannon index had a significant positive correlation with cumulative SOC mineralization. Multiple stepwise linear regression analysis showed that the SOC mineralization potential was dominantly explained by the bacterial Shannon index and operational taxonomic units (OTUs). The GW system had lower potentially mineralizable SOC and higher SOC stability. Additionally, the incubation time and cumulative SOC mineralization were well fitted by the first-order kinetic equation.

**Conclusions** LUCs significantly changed SOC mineralization characteristics and the results highlighted the important roles of the bacterial community in soil carbon cycling, which contributes to the fundamental understanding of SOC turnover regulation.

**Keywords** Land use change, Indoor incubation, Soil organic carbon mineralization, Soil enzyme activity, Bacterial alpha diversity

\*Correspondence:

Guibin Wang  
guibinwang99@163.com

<sup>1</sup> Co-Innovation Center for Sustainable Forestry in Southern China, College of Forestry, Nanjing Forestry University, 159 Longpan Road, Nanjing 210037, China



© The Author(s) 2023. **Open Access** This article is licensed under a Creative Commons Attribution 4.0 International License, which permits use, sharing, adaptation, distribution and reproduction in any medium or format, as long as you give appropriate credit to the original author(s) and the source, provide a link to the Creative Commons licence, and indicate if changes were made. The images or other third party material in this article are included in the article's Creative Commons licence, unless indicated otherwise in a credit line to the material. If material is not included in the article's Creative Commons licence and your intended use is not permitted by statutory regulation or exceeds the permitted use, you will need to obtain permission directly from the copyright holder. To view a copy of this licence, visit <http://creativecommons.org/licenses/by/4.0/>.

## Introduction

Global average temperatures are expected to increase by approximately 2–6 °C above the temperatures measured before the Industrial Revolution by 2100, and the trend of temperature increase on a global scale is parallel to the trend of changes in atmospheric carbon dioxide (CO<sub>2</sub>) (Al-Ghussain 2019; Letcher 2019). Soil organic carbon (SOC) pool is the largest organic carbon sink in the terrestrial biosphere; its extent depends on the dynamic balance between plant carbon input and microbial carbon outputs, and small changes in SOC will have a significant impact on atmospheric CO<sub>2</sub> concentration (Schmidt et al. 2011; Scharlemann et al. 2014; Bradford et al. 2016). Thus, the Intergovernmental Panel on Climate Change (IPCC) has indicated that both CO<sub>2</sub> removal and critical reductions in greenhouse gas (GHG) emissions from anthropogenic land use changes (LUCs) should be adopted to limit global warming to within 1.5 °C by 2100 (IPCC 2018; Anderson et al. 2019; Beillouin et al. 2022). Particularly, global warming will also accelerate the decomposition of SOC, thus creating a strong positive feedback with climate change (Wang et al. 2022). The soil carbon sink capacity has received extensive attention, and thus increasing SOC storage and reducing GHG emissions from soil are effective ways to address the climate change issues (Smith et al. 2016). The SOC stock exhibits significant spatial heterogeneity but is mainly affected by local-scale land use patterns and has been confirmed to be vulnerable to LUCs (Don et al. 2011).

Due to the possible transformation of soil carbon sinks and sources, a two-pronged approach, referring to broadening soil carbon input and reducing soil carbon expenditure, has become the basic strategy for carbon sequestration (Garcia-Pausas et al. 2008; Caddeo et al. 2019). LUCs driven by anthropogenic activities have induced the release of 1.6 Gt C year<sup>-1</sup> into the atmosphere in the past decade (Friedlingstein et al. 2020). However, Poeplau and Don (2013) obtained an estimate of 21 ± 13 Mg·ha<sup>-1</sup> of SOC accumulation after croplands have been changed to forests. Similarly, afforestation plays a significant role in carbon sequestration, as 39% of terrestrial ecosystem C is stored in forest ecosystems, 21.4% is stored as stand biomass and 78.6% is stored in the soil (Huang et al. 2012; Rahman et al. 2017; Zhang et al. 2021b). In general, afforested agricultural lands increase the SOC stock by 29%; this increase is relatively stable and further steadily increases with increasing tree age (Don et al. 2011). These studies have demonstrated the high C sequestration potential of afforestation, according to the aforementioned strategy, to further tap the C sequestration potential, and thoroughly elucidating the SOC output patterns is also of great significance. Namely, soil respiration is also key process affecting the

global C balance and soil nutrient cycle, which is primarily driven by the microbial decomposition of SOC, and increases or decreases in the soil respiration rate can determine whether soil serves as a “source” or “sink” (Chen et al. 2018). There is a positive correlation between soil respiration and bacterial richness in general, and thus, changes in bacterial communities following LUCs definitely alter SOC mineralization patterns, mainly because microbes are the drivers of SOC mineralization and the microbial activities directly affect the SOC turnover rate (Tardy et al. 2015; Barnett et al. 2020).

SOC mineralization reflects the SOC decomposition process and is closely related to nutrient release, CO<sub>2</sub> emission, and soil property maintenance (Li et al. 2010). The specific mechanisms underlying SOC mineralization are not yet fully understood, but some key questions regarding SOC mineralization patterns have been answered. Temperature and moisture are known to be fundamental factors affecting carbon mineralization (Huang and Hall 2017; Schlüter et al. 2022). Intermediate moisture facilitates oxygen supply and substrate diffusion, and appropriate temperatures increase microbial activity, thus affecting SOC mineralization (Wang et al. 2016; Huang and Hall 2017). Other environmental factors (e.g., soil pH, particle size distribution, nutrients, enzyme activity, and iron oxides) and anthropogenic factors (e.g., land use patterns, tillage measures, exogenous organic matter additions, and fertilization) also critically impact SOC mineralization (Autret et al. 2020; Jin et al. 2020; Wei et al. 2020; Jeewani et al. 2021; Patel et al. 2021; Zhang et al. 2021a). The abovementioned influencing factors and their interactions make it incredibly challenging to comprehensively understand SOC mineralization (Rong et al. 2021). LUCs can lead to changes in the physical, chemical and biological conditions of the soil, which will promote or inhibit the release of SOC, possibly due to the altered soil microbial activity and/or community structure, and in turn alters the SOC decomposition rate. Therefore, it is important to investigate the pathways and mechanisms of LUC affecting SOC mineralization to gain a deeper understanding of the carbon sequestration and emission reduction role of afforestation and to help achieve carbon neutrality.

Laboratory incubation methods are widely used to study SOC mineralization, although incubation at constant temperature and humidity levels cannot reflect the actual SOC mineralization patterns in the field (Moinet and Millard 2020). However, these methods can still provide a better understanding of the SOC mineralization patterns under different land use patterns from the same origin. In this study, we selected four land use patterns converted from a wheat–corn rotation system and one legacy wheat–corn rotation system in the Yellow Sea

Forest Park as the study area. We hypothesized that LUCs can affect SOC mineralization by regulating soil physicochemical properties and bacterial communities. Specifically, the main hypotheses were as follows: (1) LUCs would alter the SOC mineralization rate, i.e., lower SOC mineralization rates would be observed in the converted land use patterns than in the wheat–corn rotation system, and these differences would be controlled by certain factors among these land use patterns; and (2) the cumulative C mineralization would be controlled by different factors at different soil depths. To test these hypotheses, a 60-day incubation experiment was conducted. The results will deepen our understanding of the patterns and mechanism of SOC mineralization after LUCs in this area or similar areas.

## Materials and methods

### Study site description

The study site is located in Yellow Sea Forest Park in the city of Dongtai, Jiangsu Province (32°51′–32°52′N, 120°48′–120°50′E, 5 m above sea level), and has a subtropical monsoon climate. The region is characterized by an average annual temperature of 15.6 °C, total annual precipitation of 1061.2 mm, and a sunshine duration of 2130.5 h. The soils at the study site are classified as fluvisols according to the World Reference Base (IUSS Working Group WRB 2015). The vegetation in the park mainly consists of deciduous broad-leaved forests and evergreen broad-leaved forests, with a forest coverage rate of 66.6% and a total area of 4156.93 ha.

This study included one wheat (*Triticum aestivum*)–corn (*Zea mays*) rotation system with a >30-year history, abbreviated herein as W, and four forest land types that were wheat–corn rotation systems prior to afforestation. More details are listed in Table 1. Specifically, the ginkgo (*Ginkgo biloba*) trees at the G, GW, and GM sites were planted in 2002, and the metasequoia (*Metasequoia glyptostroboides*) trees at the M and GM sites were planted in 2010. The harvest of most crop residues (mainly wheat

and corn straw residues) at the W and GW sites occurs every year, leaving only small amounts of residue.

### Field sampling

Three 10 m × 10 m plots were randomly selected within each land use pattern, and the stand edge areas were always avoided to prevent any interactions among adjacent land use patterns and eliminate any stand edge effects. Sampling took place in mid-May 2018, when the wheat in the W and GW systems was at the beginning of the grain-filling period. According to our previous study, the SOC content decreased greatly at a depth of 20 cm (Guo et al. 2018a). Thus, stratified sampling was conducted at 0–20 cm and 20–40 cm soil depths in the abovementioned plots following an “S”-type pattern. Each sample was mixed with 10 soil cores that were randomly collected from each soil depth with a cutting ring. The sample was immediately sieved through a 2-mm screen, and fine roots and litter debris were removed. A total of 30 samples (3 replicates × 2 depths × 5 land use patterns) were collected; a small portion of the samples were placed into a dry-ice box, and the rest were placed into an ice box. After transporting them to the lab, the samples in the dry-ice box were stored in a –81 °C ultralow-temperature refrigerator for 16S rRNA sequencing. The samples in the ice box were divided into two subsamples. One subsample was then stored in a 4 °C refrigerator for SOC fraction and soil enzyme activity determination, and the other subsample was air-dried indoors for further incubation and soil analysis.

### Laboratory incubation

The incubation experiment performed herein included five land-use patterns and two soil depths with three replicates. Specifically, 15 g of sieved, air-dried soil was evenly placed in a 250-mL jar, deionized water was added to maintain 60% of the field water capacity, and three empty jars were used as controls. After preculturing for 7 days (with daily hydration during this period), a 60-day incubation experiment was conducted using an incubator

**Table 1** Basic characteristics of the study sites

| Former land use pattern | Current land use pattern  | Abbreviation | Tree age      | Main understory species                        | Density                             |
|-------------------------|---------------------------|--------------|---------------|--|-------------------------------------|
| Wheat–corn system       | Ginkgo plantation         | G            | 16            | <i>Oxalis corniculata</i> , <i>Ipomoea nil</i> | 3 m × 3 m                           |
|                         | Wheat–corn system         | W            | –             | Wheat, corn                                    | –                                   |
|                         | Metasequoia plantation    | M            | 7             | Fern   | 0.8 m × 0.8 m                       |
|                         | Ginkgo–wheat–corn system  | GW           | 16            | Wheat, corn                                    | 2 m × 8 m                           |
|                         | Ginkgo–metasequoia system | GM           | 16 (G), 7 (M) | Fern   | 2 m × 8 m (G),<br>0.8 m × 0.8 m (M) |

maintained at a constant temperature of 25°C. A small beaker containing 15 mL 1 M NaOH was used to absorb the released CO<sub>2</sub>. The beakers were removed to determine the absorbed CO<sub>2</sub> at different intervals (at exactly 1, 2, 3, 4, 5, 6, 7, 9, 11, 13, 15, 18, 21, 24, 27, 30, 33, 36, 39, 42, 46, 50, 54, 58, and 60 days) during the incubation process. Then, excess 1 M BaCl<sub>2</sub> was added to precipitate CO<sub>3</sub><sup>2-</sup>, and the residual NaOH in the solution was titrated with 1 M HCl in the presence of excess BaCl<sub>2</sub>. Cumulative mineralization was expressed in mg CO<sub>2</sub>-C kg<sup>-1</sup> dry soil (Li et al. 2022a). After each CO<sub>2</sub> release measurement, the jar was kept open for 2 h to ensure sufficient O<sub>2</sub> availability for soil microbial respiration. The SOC mineralization ratio was calculated as the cumulative CO<sub>2</sub> emissions divided by the SOC content (g CO<sub>2</sub>-C g<sup>-1</sup> SOC), and the metabolic quotient (*q*CO<sub>2</sub>, mg CO<sub>2</sub>-C g<sup>-1</sup> MBC h<sup>-1</sup>) was calculated according to Xiao et al. (2017):

$$q\text{CO}_2 = \Sigma C_i / (\text{MBC} \cdot T),$$

where  $\Sigma C_i$  is the cumulative CO<sub>2</sub> emission (mg CO<sub>2</sub>-C kg<sup>-1</sup>), MBC is the soil MBC content (g kg<sup>-1</sup>), and *T* is the incubation time.

### Soil analysis

Classical approaches were employed to determine the pH, bulk density, SOC, total nitrogen (TN), total phosphorus (TP), and total potassium (TK) contents of the soil samples. Briefly, the soil pH was determined using the potentiometric method (soil:water ratio of 1:2.5, w/v); the ring knife method was used to determine the bulk density; SOC was determined using the potassium dichromate oxidation external heating method; TN was determined using the semimicro Kjeldahl method; TP was determined through sodium hydroxide melting molybdenum antimony colorimetry; and TK was determined using the sodium hydroxide melting flame photometer method. The results of these indices and the soil bacterial community composition and diversity have been published in Guo et al. (2021). The analysis methods for microbial biomass carbon (MBC), dissolved organic carbon (DOC), and readily oxidizable organic carbon (ROC) were previously described in Guo et al. (2018a).

The soil urease, alkaline phosphatase, and catalase activities were determined based on the methods of Guan (1986). Briefly, the soil alkaline phosphatase activity was determined by the sodium benzene phosphate colorimetric method, soil urease activity was determined by the sodium diphenyl phosphate colorimetric method, and catalase activity was determined by the potassium permanganate titration method.

### Kinetic modeling

A first-order kinetic model was used to calculate the key parameters of SOC mineralization, and the equation can be expressed as follows (Li et al. 2022a):

$$C_t = C_0 (1 - e^{-kt}),$$

where *t* is the incubation time, *C<sub>t</sub>* is the accumulated amount of SOC mineralized at time *t*, *k* is the mineralization rate constant, and *C<sub>0</sub>* is the potentially mineralizable SOC. In addition, the proportion of potentially mineralizable SOC to total SOC can be calculated with the following formula: *C<sub>0</sub>*/SOC.

### Statistical analysis

SPSS software (version 20.0, Chicago, USA) was used to calculate the mean and standard deviations of the triplicate samples. Two-way analysis of variance (ANOVA) was used to analyze the effects of different land-use patterns and soil depths on the resulting SOC fractions, enzyme activity, and mineralization-relevant indicators. Before conducting ANOVA analyses, the distribution normality and variance uniformity were tested. Pearson's correlation analysis was performed to analyze the correlations between the cumulative SOC mineralization and soil SOC fractions, physicochemical properties, enzyme activity, and bacterial α-diversity indices. The first-order kinetics fitting curve was derived using Origin software (version 2018, Northampton, USA).

## Results

### SOC and fractions and extracellular soil enzyme activity

Compared with the W system, LUCs increased the MBC by 15.41–77.02% and by 87.50–156.31% at the 0–20 cm and 20–40 cm soil depths, respectively. Only the GW system at the 0–20 cm soil depth and the M system at the 20–40 cm soil depth exhibited higher ROC contents than those in the W system, with an increase by 25.86% and 43.72%, respectively. The DOC contents in the G system were highest at both the 0–20 cm and 20–40 cm soil depths, reaching 261.16 and 283.72 mg·kg<sup>-1</sup>, respectively. The two-way ANOVA results showed that LUCs had significant influences on the MBC, ROC, and DOC, while the soil depth significantly influenced the MBC and ROC contents (Fig. 1, *P* < 0.05). The lowest urease activity was found in the W system at the 0–20 cm soil depth, only 14.14–29.20% of other systems. The GW system had 114.66% and 10.15% higher alkaline phosphatase activity than the W system at the 0–20 cm and 20–40 cm soil depths, respectively. The two-way ANOVA results showed that LUCs exerted a significant influence on the alkaline phosphatase and catalase activity and that soil

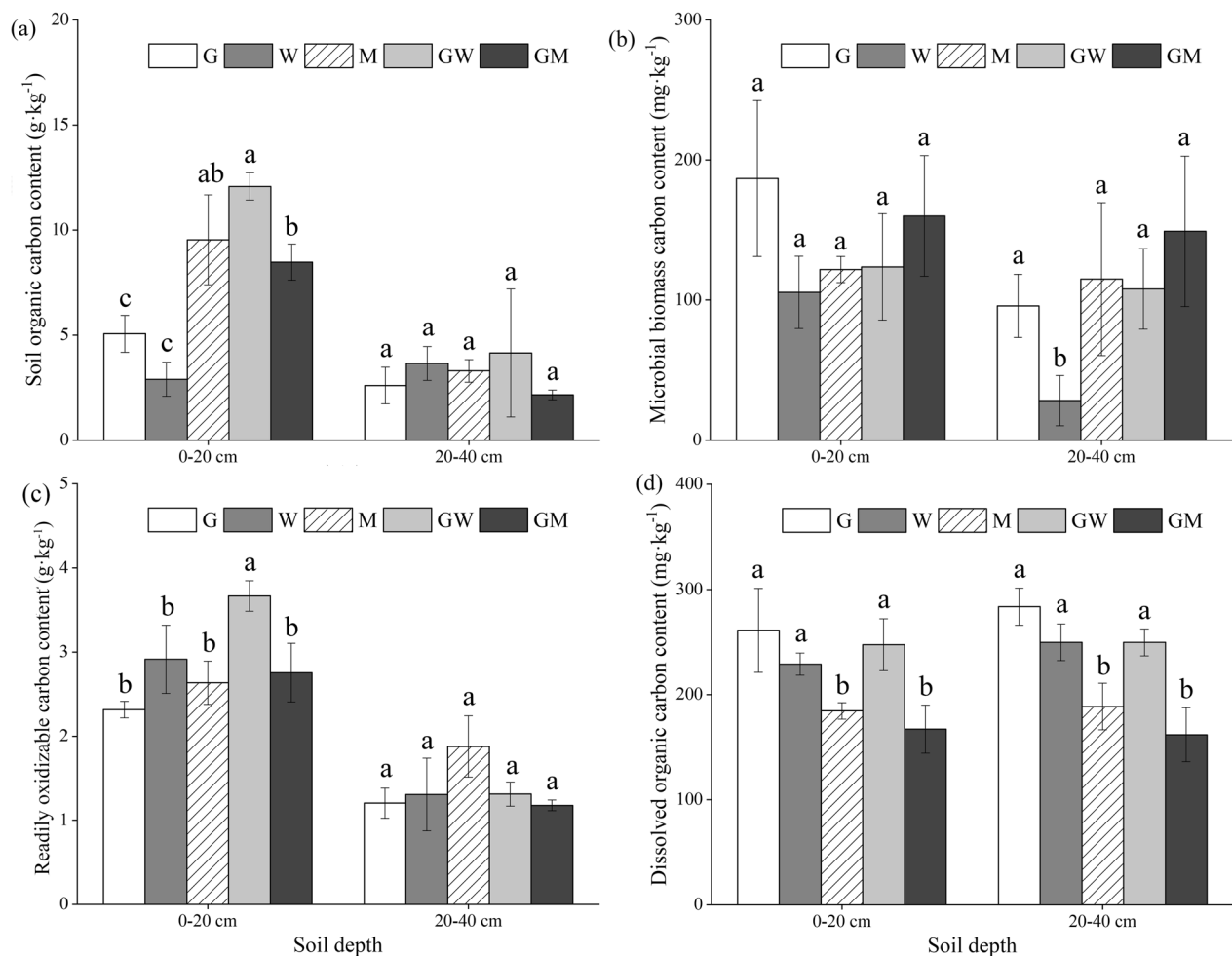


**Fig. 1** Contents of soil organic carbon and fractions of different land-use patterns at 0–20 cm and 20–40 cm soil depths. G, W, M, GW and GM represent ginkgo plantations, wheat–corn systems, metasequoia plantations, ginkgo–wheat–corn systems and ginkgo–metasequoia systems, respectively (values are the means  $\pm$  standard deviations,  $n = 3$ ). Different lowercase letters indicate significant differences among different land use patterns at the same soil depth ( $P < 0.05$ )

depth significantly influenced the urease, alkaline phosphatase and catalase activity (Fig. 2,  $P < 0.05$ ).

### Cumulative SOC mineralization

During this 60-day indoor incubation experiment, the cumulative SOC mineralization significantly varied among the five land-use patterns (Fig. 3). At the 0–20 cm depth, the cumulative mineralization followed the order of  $M > G > GM > W > GW$ , and the cumulative amount was highest in the M system (118.80 mg  $\text{CO}_2\text{-C}\cdot\text{kg}^{-1}$  dry soil), which was 1.17 times that of W system and 1.20 times that of GW system. The cumulative SOC mineralization amount of W and GW systems was similar and significantly lower than those in other systems ( $P < 0.05$ ). At the 20–40 cm depth, the cumulative SOC mineralization followed the order of  $G > W > GM > M > GW$ , and the cumulative amount under the G system was 78.08

mg  $\text{CO}_2\text{-C}\cdot\text{kg}^{-1}$  dry soil, which was 1.29 times that of the GW system. The cumulative SOC mineralization decreased with increasing soil depth, with the M system showing the greatest decrease of 55.26 mg of  $\text{CO}_2\text{-C}\cdot\text{kg}^{-1}$  dry soil and the W system showing the smallest decrease of 31.13 mg  $\text{CO}_2\text{-C}\cdot\text{kg}^{-1}$  dry soil. The Pearson correlation analysis results showed that the cumulative SOC mineralization was significantly positively correlated with ROC, SOC ( $R^2 = 0.764$ ,  $P = 0.01$ ;  $R^2 = 0.643$ ,  $P = 0.045$ ), MBC, and C/N ( $R^2 = 0.467$ ,  $P = 0.174$ ; Fig. 4).

### SOC mineralization rate

All land use patterns showed rapid increases and great fluctuations in SOC mineralization rate during the initial incubation phase; maximum rates were observed at 15–18 d (for the 0–20 cm depth) and at 9 d (for the 20–40 cm depth), and after that the efflux gradually

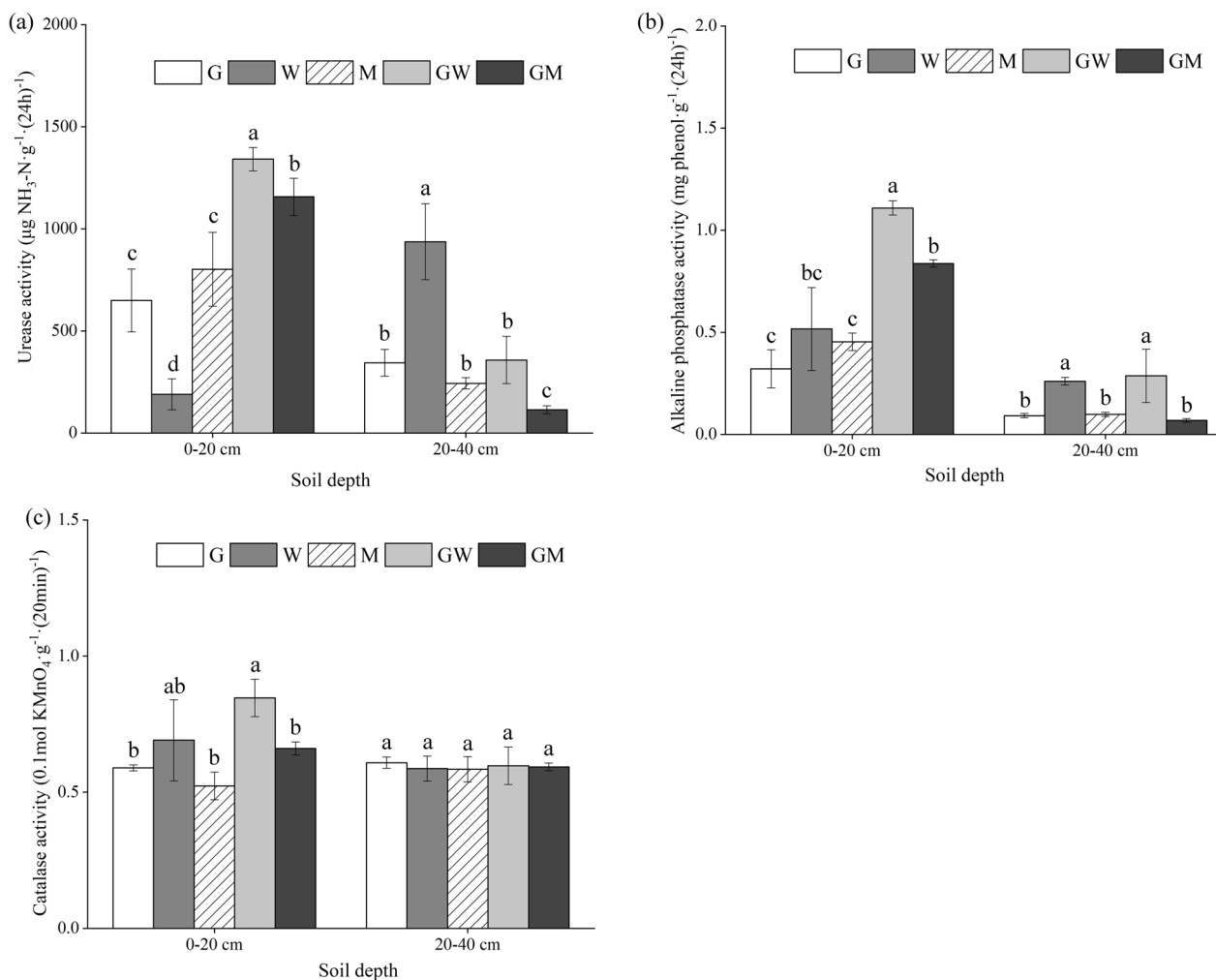


**Fig. 2** Soil urease (a), alkaline phosphatase (b), and catalase (c) activity of different land use patterns at 0–20 cm and 20–40 cm soil depths (values are the means  $\pm$  standard deviations,  $n=3$ ). Different lowercase letters indicate significant differences among land use patterns at the  $P=0.05$  level

decreased and then stabilized (Fig. 5). At the 0–20 cm depth, the maximum rate measured under the M system was  $13.47\text{ mg CO}_2\text{-C}\cdot\text{kg}^{-1}\cdot\text{d}^{-1}$ , which was 94.86% and 121.18% higher than those obtained under the W and G systems, respectively. At the 20–40 cm depth, the maximum rate measured under the M system was  $8.79\text{ mg CO}_2\text{-C}\cdot\text{kg}^{-1}\cdot\text{d}^{-1}$ , which was 7.67% and 36.69% higher than those obtained under the W and G systems, respectively. The average SOC mineralization rates showed significant differences among the different land-use patterns and between the two soil depths ( $P<0.05$ ), as well as the SOC mineralization ratio and the microbial metabolic quotient (Fig. 6). The mineralization ratio was highest in the W system and lowest in the GW system, and the W system had the highest microbial metabolic quotient, reaching  $41.42\text{ mg CO}_2\text{-C}\cdot\text{g}^{-1}\text{ MBC}\cdot\text{h}^{-1}$ .

### SOC mineralization fitting parameters

The first-order kinetic equation of incubation time and cumulative SOC mineralization fitted well, with fitting coefficients ( $R^2$ ) ranging from 0.931 to 0.986 (Table 2). The potentially mineralizable SOC ( $C_0$ ) values ranged from 62.70 to  $148.04\text{ mg}\cdot\text{kg}^{-1}$ . The M and G systems had the highest  $C_0$  values at the 0–20 cm and 20–40 cm soil depths ( $148.04\text{ mg}\cdot\text{kg}^{-1}$  and  $118.46\text{ mg}\cdot\text{kg}^{-1}$ , respectively), while the GW system had the lowest  $C_0$  value at both soil depths. The topsoil layer always had higher  $C_0$  values and lower mineralization rate constants ( $k$ ) than the 20–40 cm depth. The dynamics of cumulative SOC mineralization following incubation time at the 0–20 cm and 20–40 cm soil depths under different land-use patterns and the corresponding kinetic simulations are shown in Fig. 7.

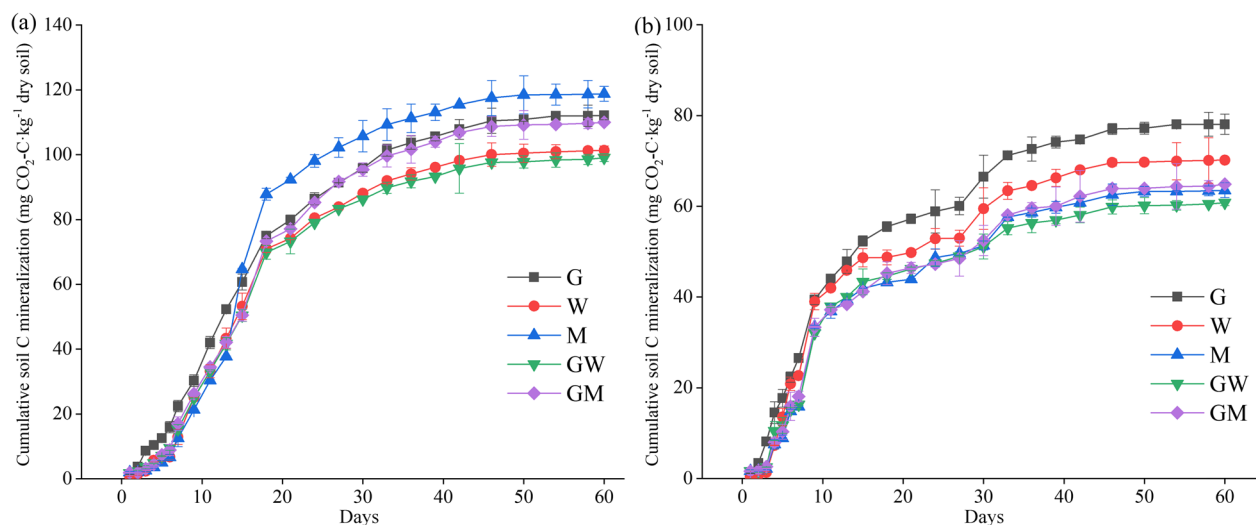


**Fig. 3** Cumulative SOC mineralization under different land-use patterns during 60-day incubation at 25 °C (values are the means  $\pm$  standard deviations,  $n=3$ ). **a** Cumulative SOC mineralization at 0–20 cm soil depth; **b** cumulative SOC mineralization at 20–40 cm soil depth

### Relationships between cumulative SOC mineralization and soil properties, enzyme activity, and soil bacterial $\alpha$ -diversity

Relationships between the cumulative SOC mineralization and the soil properties, enzyme activity, and soil bacterial  $\alpha$ -diversity were analyzed (Table 3). The soil pH and bulk density were significantly negatively correlated with the cumulative SOC mineralization ( $P < 0.05$ ). The soil bacterial Shannon index was significantly positively correlated with cumulative SOC mineralization ( $P < 0.05$ ).

Multiple stepwise linear regressions were used to further analyze the relationships between the cumulative SOC mineralization and soil properties, enzyme activity, and soil bacterial  $\alpha$ -diversity indices (Table 4). The SOC mineralization potential was well explained by the Shannon index (68.9%, Model 1) and jointly explained by the Shannon index and OTUs (83.5%, Model 2).

### Discussion

Overall, reducing the  $\text{CO}_2$  expenditure (a lower SOC mineralization level) in the soil is always effective strategy for combating climate change (Montagnini and Nair 2004; Hontoria et al. 2016). LUCs always lead to changes in the physical, chemical and biological conditions of the soil, which may promote or inhibit the SOC release. Thus, exploring the SOC mineralization rules and their variations among land use patterns is critical for accurately predicting SOC dynamics and the C sequestration potential following LUCs. Generally, the results obtained in our study were partly contrary to our first hypothesis but they verified the second hypothesis. Exactly, different LUC patterns had diverse impacts on SOC mineralization

The G, M, and GM systems had significantly higher cumulative SOC mineralization values than the other two systems in the 0–20 cm soil layer. GW had the highest SOC content and lowest cumulative SOC mineralization, indicating the small proportion of substrate available for microbial decomposition (Zhang et al. 2021a). Another explanation is that the wheat straws generally have higher C/N ratio and more recalcitrant C components, which hindered the litter decomposition and C mineralization (Guo et al. 2018b). The cumulative SOC mineralization at the 0–20 cm and 20–40 cm soil depths after 60-day incubation ranged from 99.08–118.80  $\text{mg CO}_2\text{-C}\cdot\text{kg}^{-1}$  dry soil and from 60.79–78.08  $\text{mg CO}_2\text{-C}\cdot\text{kg}^{-1}$  dry soil, respectively. The mineralization ratio was relatively low, likely because the incubated soils represented original soils without any addition of organic substrates, such as straw or biochar (Liu et al. 2019; Roy et al. 2022). Afforestation leads to changes of aboveground vegetation, root distribution and density, litter quality and quantity, and then affects the microbial community composition, thus resulting in SOC and fractions variations, all of these will affect the SOC mineralization patterns, especially in the topsoil layer (Tian et al. 2016; Chavarria et al. 2018; Guo et al. 2021). Likewise, Chia et al. (2017) reported that a greater labile SOC pool and larger soil microbial populations enhanced SOC mineralization, especially in the first 10 years of afforestation (Chen et al. 2016). The gradually increasing proportion of recalcitrant SOC (aromatic-like substances) maintains pace with the forest stand development, which may lead to a reduction in the SOC mineralization rate (Huang et al. 2019). Thus, the greater cumulative SOC mineralization in the M system

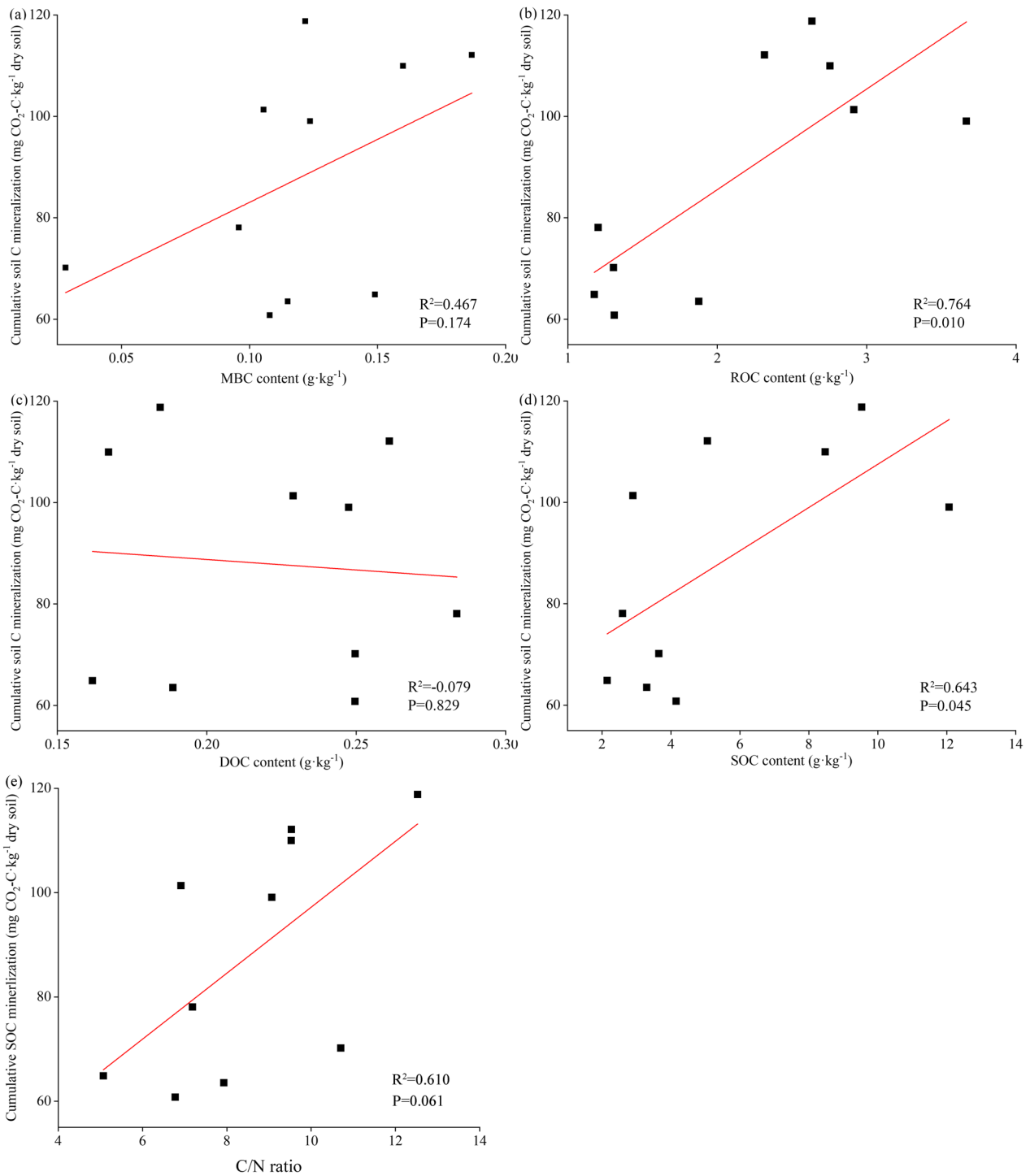


**Fig. 4** Pearson correlations between the cumulative SOC mineralization and microbial biomass carbon (a), and readily oxidizable organic carbon (b), and dissolved organic carbon (c), and soil organic carbon (d), and ratio of soil organic carbon and total nitrogen (e)

might be ascribed to the higher substrate availability and the resultant increases of microbial biomass and activity in this system, which is conducive to microbial decomposition. In our study, there were significant differences

in the cumulative SOC mineralization between the two soil depths, with lower values in the subsoil layer (Neculman et al. 2021). Liang et al. (2018) suggested that the lower cumulative SOC mineralization in subsoils may

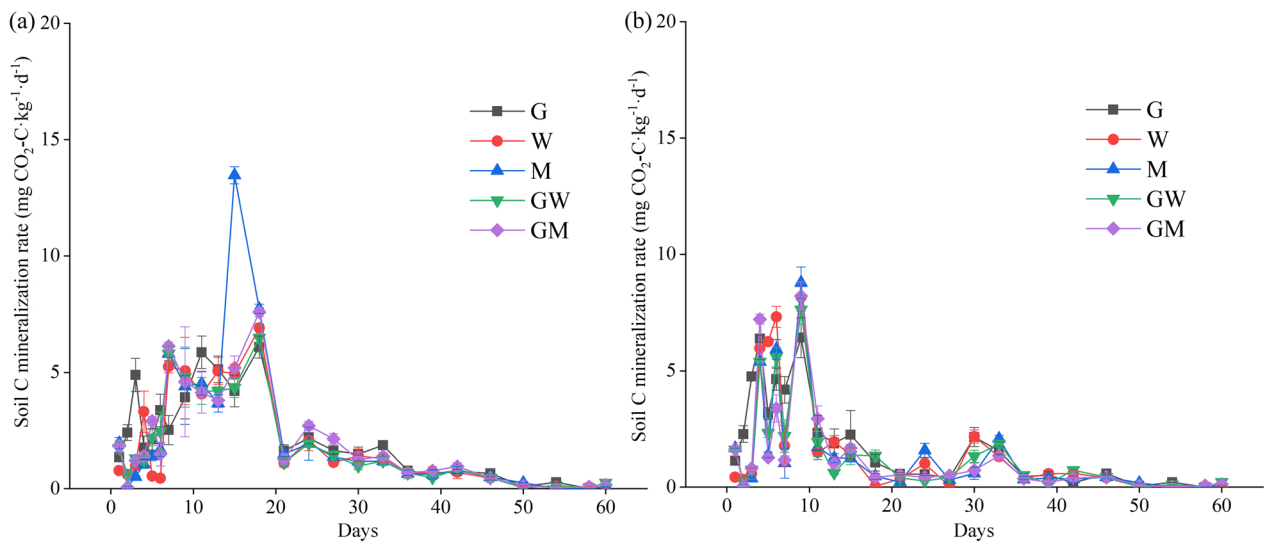


**Fig. 5** SOC mineralization rate under different land-use patterns (values are the means  $\pm$  standard deviations,  $n = 3$ ). **a** SOC mineralization rate at 0–20 cm soil depth, **b** SOC mineralization rate at 20–40 cm soil depth

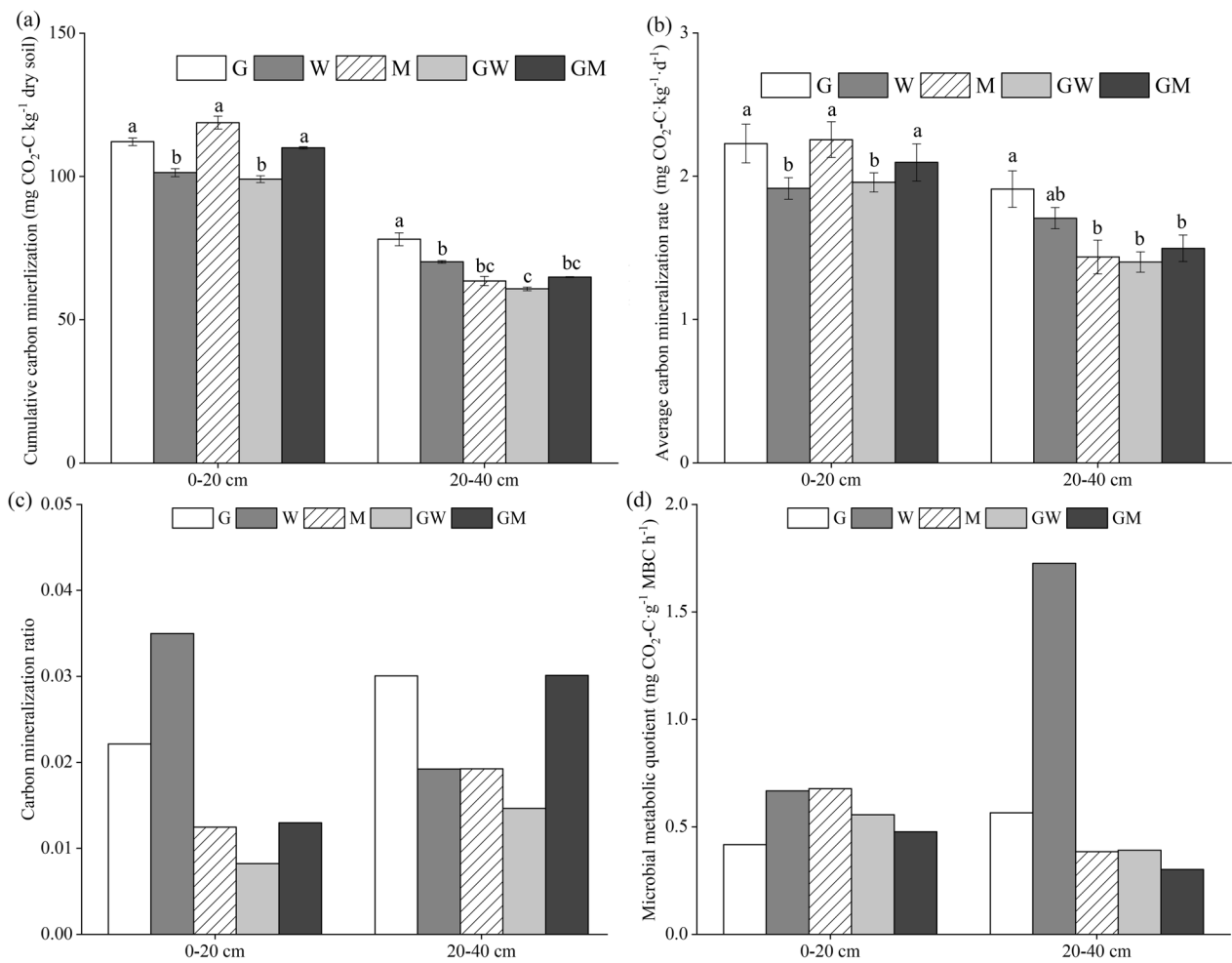


**Fig. 6** Mineralization index of organic carbon under different land-use patterns. **a** Cumulative mineralization amount, **b** average mineralization rate, **c** SOC mineralization ratio, and **d** microbial metabolic quotient

**Table 2** Kinetic parameters of organic carbon mineralization in the topsoil and subsoil under different land use patterns

|          | $C_0$ (mg·kg <sup>-1</sup> ) | $C_0$ /SOC (%) | $K$ (d <sup>-1</sup> ) | $R^2$   |
|----------|------------------------------|----------------|------------------------|---------|
| 0–20 cm  |                              |                |                        |         |
| G        | 130.65 ± 6.00                | 2.58           | 0.0399 ± 0.0039        | 0.977** |
| W        | 122.82 ± 9.35                | 4.24           | 0.0363 ± 0.0057        | 0.955** |
| M        | 148.04 ± 15.28               | 1.55           | 0.0345 ± 0.0071        | 0.931** |
| GW       | 118.46 ± 8.23                | 0.98           | 0.0375 ± 0.0054        | 0.959** |
| GM       | 136.58 ± 10.70               | 1.61           | 0.0339 ± 0.0052        | 0.959** |
| 20–40 cm |                              |                |                        |         |
| G        | 80.83 ± 1.69                 | 3.11           | 0.0609 ± 0.0035        | 0.986** |
| W        | 72.89 ± 2.60                 | 2.00           | 0.0599 ± 0.0058        | 0.964** |
| M        | 67.28 ± 2.50                 | 2.04           | 0.0545 ± 0.0052        | 0.968** |
| GW       | 62.70 ± 1.98                 | 1.51           | 0.0628 ± 0.0055        | 0.968** |
| GM       | 68.23 ± 2.31                 | 3.17           | 0.0544 ± 0.0048        | 0.973** |

The  $k$  is the mineralization rate constant;  $C_0$  is the potentially mineralizable organic carbon content in the soil; and  $C_0$ /SOC is the proportion of potentially mineralizable organic carbon to total organic carbon

be due to delayed mineralization rather than the provisioning of greater protection through mineral binding or a lack of metabolic potential. In our study, cumulative SOC mineralization was found to be positively correlated with ROC, SOC, MBC, and C/N, indicating that labile organic C pools are an important factor determining the soil CO<sub>2</sub> emission (Liu et al. 2019; Lu et al. 2020; Zhang et al. 2021a). Despite the decreasing proportion of labile C pools following afforestation, the total SOC amount increased, leading to a lower mineralization ratio but increased cumulative SOC mineralization. Moreover, a poor correlation between the cumulative SOC mineralization and DOC was also observed in Entisols by Ma et al. (2019); their finding was partly explained by the relatively high proportion of recalcitrant compounds in the DOC. The microbial biomass and substrate availability are always the dominant factors of SOC mineralization following afforestation. Conversely, the increased microbial growth and extracellular enzyme activities will facilitate the degradation of SOC. As demonstrated by Barnett et al. (2022), LUCs have profound impacts on the soil C cycle path through the microbial food web, and these differences always linked to C mineralization performance. Microbial biomass influences C cycling by altering resource pathways between microbes with diverse life history strategies, in which low-biomass soils favor fast-growing organisms that exhibit repeated cycles, while high-biomass soils favor microbes that adapt to efficient resource access and less dynamic growth cycles. These provide a framework for improving our understanding of microbially mediated terrestrial carbon cycling.

In line with previous studies, marked peaks and fluctuations in the mineralization rate were also observed in

our incubation experiments, regardless of the soil properties or land use patterns (Zhou et al. 2013; Fanin and Bertrand 2016). The results showed that the maximum mineralization rate at the 0–20 cm soil depth was higher than that at the 20–40 cm soil depth, and great differences were observed among the different land-use patterns. Notably, greater litter and root inputs and higher microbial activities occurred in the topsoil layer, thus affecting soil particle aggregation and SOC quality and quantity and resulting in relatively high cumulative SOC mineralization in the topsoil layer (Chavarria et al. 2018; Nadal-Romero et al. 2016). The diverse SOC mineralization rates were directly or indirectly caused by long-term changes in biotic and abiotic factors and their interactions following LUCs. The relatively higher SOC mineralization rates in the afforested systems, especially at the subsoil depths, could be partially explained by the greater root biomass and deeper root distribution in these land use types (Kuzakov and Xu 2013). Previous studies have shown that the main drivers of SOC changes in different tillage systems are the quantity and quality of organic inputs rather than any change in soil tillage practices, which, in fact, may not affect the specific SOC mineralization rates (Autret et al. 2020). The degradation of labile C contributed to the rapid increase in the SOC mineralization rate observed over the first 9 or 15 days at the 20–40 cm or 0–20 cm soil depths, and the subsequent reductions in the active C pool proportion led to subsequent declines in the SOC mineralization rate (Munda et al. 2018). Hence, soils with low available SOC contents reached the maximal SOC mineralization rates rapidly, while soils with high available SOC contents require a longer period to consume these substrates, which would result in a lag before peak C mineralization is achieved. If the process was further divided into two stages, the initial period (days 0–33) mainly relied on the colonization ability of microbial communities and active C pool mineralization, while the second phase was mainly constrained by the labile C availability in the soil (Luo et al. 2017; Tang et al. 2018). It can also be interpreted as the mineralization patterns consist of the first phase of readily available SOC decomposition and the second phase of secondary transformations of microbial products (Barnett et al. 2022). Growing evidence has shown that soil physicochemical properties and microbial communities strongly affect the SOC mineralization rate (You et al. 2014; Fabian et al. 2017). The  $qCO_2$  level has been proven to be a significant indicator of the microbial assimilation efficiency; a relatively high  $qCO_2$  indicates a low utilization efficiency of carbon sources. Here, the  $qCO_2$  levels at both soil depths in the W system were higher than those in the other systems, demonstrating that more carbon sources are used by microorganisms for respiration

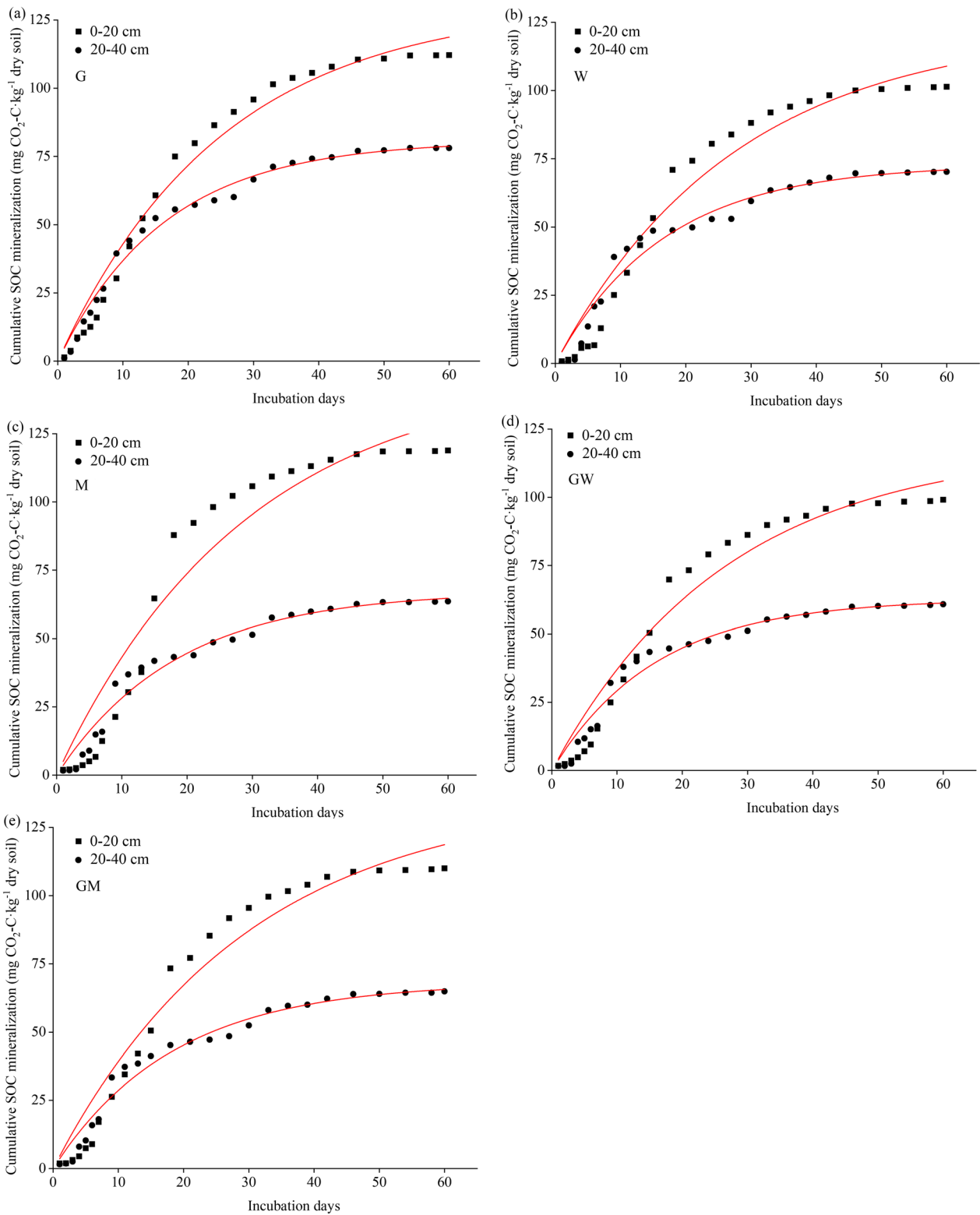


**Fig. 7** Changes in SOC cumulative mineralization with incubation time and dynamic simulation based on the first-order kinetic equation at 0–20 cm and 20–40 cm soil depths under different land-use patterns

**Table 3** Pearson's correlation analysis results between the cumulative SOC mineralization and soil properties, enzyme activity, and soil bacterial  $\alpha$ -diversity levels

| Variables            | Cumulative SOC mineralization |                |
|----------------------|-------------------------------|----------------|
|                      | <i>r</i>                      | <i>P</i> value |
| pH                   | <b>− 0.811**</b>              | <b>0.004</b>   |
| BD                   | <b>− 0.640*</b>               | <b>0.046</b>   |
| TN                   | 0.501                         | 0.14           |
| TP                   | 0.592                         | 0.071          |
| TK                   | 0.017                         | 0.963          |
| Shannon              | <b>0.850**</b>                | <b>0.002</b>   |
| OTUs                 | 0.455                         | 0.187          |
| ACE                  | 0.162                         | 0.655          |
| Chao                 | 0.163                         | 0.653          |
| Urease               | 0.519                         | 0.124          |
| Alkaline phosphatase | 0.612                         | 0.06           |
| Catalase             | 0.191                         | 0.596          |

The bold values reflect the significant correlation between the cumulative SOC mineralization and specific soil property (\* $0.01 < P < 0.05$ , \*\* $P < 0.01$ )

BD indicates bulk density; TN indicates total nitrogen; TP indicates total phosphorus; TK indicates total potassium; the soil bacterial  $\alpha$ -diversity, operational taxonomic units (OTUs), Shannon's diversity index, ACE, and Chao values are also listed

rather than sustaining microbial development in this system, thus limiting the development of microbial communities and inhibiting soil quality improvements and SOC sequestration (Huang et al. 2019). Accordingly, SOC mineralization was directly promoted by increased microbial C assimilation, and the relative abundances of genes associated with labile C decomposition may have also played important roles (Wang et al. 2023).

Additionally, the first-order kinetic equation employed herein distinctly showed the amount of C lost at our study site. Furthermore, the relatively low  $C_0$ /SOC values reflected the low mineralization rate and high SOC sequestration capacity to a certain extent (Sarkar et al. 2021). The decreased  $C_0$ /SOC in the plantations and agroforestry systems after LUCs indicated that the afforestation promoted SOC transformation but reduced soil

C loss due to mineralization. In our study, the cumulative SOC mineralization was found to be significantly correlated to the soil pH, bulk density, and bacterial Shannon index. When relatively high pH values were measured in the alkaline range, they always induced a reduction in microbial activity and then limited the decomposition of plant-derived macromolecules (Yang et al. 2022). Furthermore, in agreement with our results, Hu et al. (2020) indicated that the soil pH, texture and microbial communities greatly contribute to the persistence of SOM, especially the portion controlled by microorganisms. Thus, the significant effects of soil physicochemical properties, soil substrates, and soil bacterial communities and their interactions on the cumulative SOC mineralization and mineralization rate emphasize the complex regulatory mechanisms associated with biotic and abiotic factors on the accumulation and turnover of soil C (You et al. 2016; Tang et al. 2018). The results of the multiple stepwise linear regression analysis further showed that the SOC mineralization potential could be well explained by the Shannon index (68.9%, Model 1) and jointly explained by the Shannon index and OTUs (83.5%, Model 2); these findings corroborated those of Li et al. (2022b), who reported that the SOC mineralization is mainly controlled by the bacterial community composition but may also be regulated by the organic C supply in the subsoil. The bacterial community composition and networks affect enzyme activity involved in the degradation of C compounds and SOC mineralization (Wang et al. 2021). Regardless of the analyzed system or soil layer, the available organic C is exhausted by the late incubation stage, leading to changes in the abundances of keystone species and thereby increasing the utilization of refractory organic matters (Blagodatskaya and Kuzyakov 2008). To obtain empirical evidence of the relationships between the microbial community and SOC mineralization, sequencing and functional microbial diversity analyses should be further studied, especially the relationships between abundance of copiotrophic/oligotrophic taxa and the mineralization patterns, and the microbial variations during the incubation (Wu et al. 2023). Furthermore, due to the important role of fungi in recalcitrant

**Table 4** Multiple stepwise regression analysis results

| Dependent variable            | Model | Explanatory variable | Coefficient | Standard deviation | <i>T</i> value | <i>P</i> value | Adjusted $R^2$ |       |
|-------------------------------|-------|----------------------|-------------|--------------------|----------------|----------------|----------------|-------|
| Cumulative SOC mineralization | 1     | Constant             | − 802.89    | 194.913            | − 4.12         | 0.003          | 0.689          |       |
|                               |       | Shannon              | 130.21      | 28.486             | 4.57           | 0.002          |                |       |
|                               | 2     | Constant             | − 1135.47   | 183.972            | − 6.17         | 0.0003         |                | 0.835 |
|                               |       | Shannon              | 209.965     | 34.897             | 6.02           | 0.0005         |                |       |
|                               |       | OTUs                 | − 0.078     | 0.027              | − 2.84         | 0.025          |                |       |
|                               |       |                      |             |                    |                |                |                |       |

SOC decomposition, further studies should be conducted to verify their assumed role (Dong et al. 2023).

## Conclusion

Our results confirmed that both LUCs and soil depths significantly affected the SOC mineralization rate, while different LUC patterns had diverse impacts on SOC mineralization, and the cumulative mineralization in the metasequoia plantation and ginkgo plantation was significantly higher than those in the wheat–corn and ginkgo–wheat–corn systems. The greater cumulative SOC mineralization in the topsoil was probably due to the greater organic C supply and the diverse bacterial community structure. Through the kinetic modeling, we also found that the ginkgo–wheat–corn system had lower potentially mineralizable organic C and higher SOC stability, which indicated its greater C sequestration potential and the specific mechanism that needs to be thoroughly studied in situ. Moreover, SOC mineralization potential was well explained by the bacterial Shannon index and the OTUs, revealing the response of SOC mineralization to bacterial communities. Overall, the results showed that LUCs significantly changed the SOC mineralization characteristics and highlighted the important roles of microbial processes driving soil carbon cycle, which contributes to the fundamental understanding of SOC turnover regulation. Our findings provide a scientific basis for understanding the C budget in this area, but the mechanisms of such CO<sub>2</sub> emission and the growth strategies of microorganisms warrant further investigation.

## Acknowledgements

This work was supported by the Jiangsu Special Fund on Technology Innovation of Carbon Dioxide Peaking and Carbon Neutrality (BE2022420), the Natural Science Foundation of Jiangsu Province (No. BK20210609), and the Priority Academy Program Development of Jiangsu Higher Education Institution (PAPD).

## Author contributions

JG and GW planned and designed the research. WX, JQ and JG performed experiments, conducted field work, and analyzed the data. JG wrote the first draft of the manuscript. GW reviewed and edited the draft. All authors commented on previous versions of the manuscript and have read and approved the final manuscript.

## Availability of data and materials

The data and materials supporting the conclusions of this study are included within the article. Data can be obtained from corresponding author upon reasonable request.

## Declarations

### Ethics approval and consent to participate

Not applicable.

### Consent for publication

Not applicable.

## Competing interests

The authors have no relevant financial or non-financial interests to disclose.

Received: 17 April 2023 Accepted: 4 August 2023

Published online: 28 August 2023

## References

- Al-Ghussain L (2019) Global warming: review on driving forces and mitigation. *Environ Prog Sustain Energy* 38:13–21. <https://doi.org/10.1002/ep.13041>
- Anderson CM, DeFries RS, Litterman R, Matson PA, Nepstad DC, Pacala S, Schlesinger WH, Shaw MR, Smith P, Weber C, Field CB (2019) Natural climate solutions are not enough. *Science* 363:933–934. <https://doi.org/10.1126/science.aaw2741>
- Autret B, Guillier H, Pouteau V, Mary B, Chenu C (2020) Similar specific mineralization rates of organic carbon and nitrogen in incubated soils under contrasted arable cropping systems. *Soil Tillage Res* 204:104712. <https://doi.org/10.1016/j.still.2020.104712>
- Barnett SE, Youngblut ND, Buckley DH (2020) Soil characteristics and land-use drive bacterial community assembly patterns. *FEMS Microbiol Ecol* 96:fiz194. <https://doi.org/10.1093/femsec/fiz194>
- Barnett SE, Youngblut ND, Buckley DH (2022) Bacterial community dynamics explain carbon mineralization and assimilation in soils of different land-use history. *Environ Microbiol* 24:5230–5247. <https://doi.org/10.1111/1462-2920.16146>
- Beillouin D, Cardinael R, Berre D, Boyer A, Corbeels M, Fallot A, Feder F, Demeunois J (2022) A global overview of studies about land management, land-use change, and climate change effects on soil organic carbon. *Glob Change Biol* 28:1690–1702. <https://doi.org/10.1111/gcb.15998>
- Blagodatskaya E, Kuzyakov Y (2008) Mechanisms of real and apparent priming effects and their dependence on soil microbial biomass and community structure: critical review. *Biol Fertil Soils* 45:115–131. <https://doi.org/10.1007/s00374-008-0334-y>
- Bradford MA, Wieder WR, Bonan GB, Fierer N, Raymond PA, Crowther TW (2016) Managing uncertainty in soil carbon feedbacks to climate change. *Nat Clim Change* 6:751–758. <https://doi.org/10.1038/nclimate3071>
- Caddeo A, Marras S, Sallustio L, Spano D, Sirca C (2019) Soil organic carbon in Italian forests and agroecosystems: estimating current stock and future changes with a spatial modelling approach. *Agric For Meteorol* 278:107654. <https://doi.org/10.1016/j.agrformet.2019.107654>
- Chavarria DN, Pérez-Brandan C, Serri DL, Meriles JM, Restovich SB, Andriulo AE, Jacquelin L, Vargas-Gil S (2018) Response of soil microbial communities to agroecological versus conventional systems of extensive agriculture. *Agric Ecosyst Environ* 264:1–8. <https://doi.org/10.1016/j.agee.2018.05.008>
- Chen Y, Chen G, Robinson D, Yang Z, Guo J, Xie J, Fu S, Zhou L, Yang Y (2016) Large amounts of easily decomposable carbon stored in subtropical forest subsoil are associated with r-strategy-dominated soil microbes. *Soil Biol Biochem* 95:233–242. <https://doi.org/10.1016/j.soilbio.2016.01.004>
- Chen J, Luo Y, García-Palacios P, Cao J, Daca M, Zhou X, Li J, Xia J, Niu S, Yang H, Shelton S, Guo W, van Groenigen KJ (2018) Differential responses of carbon-degrading enzymes activities to warming: implications for soil respiration. *Global Change Biol* 24:4816–4826. <https://doi.org/10.1111/gcb.14394>
- Chia RW, Kim DG, Yimer F (2017) Can afforestation with *Cupressus lusitanica* restore soil C and N stocks depleted by crop cultivation to levels observed under native systems? *Agric Ecosyst Environ* 242:67–75. <https://doi.org/10.1016/j.agee.2017.03.023>
- Don A, Schumacher J, Freibauer A (2011) Impact of tropical land-use change on soil organic carbon stocks—a meta-analysis. *Glob Change Biol* 17:1658–1670. <https://doi.org/10.1111/j.1365-2486.2010.02336.x>
- Dong X, Liu C, Wu X, Man H, Wu X, Ma D, Li M, Zang S (2023) Linking soil organic carbon mineralization with soil variables and bacterial communities in a permafrost-affected tussock wetland during laboratory incubation. *Catena* 221:106783. <https://doi.org/10.1016/j.catena.2022.106783>
- Fabian J, Zlatanovic S, Mutz M, Premke K (2017) Fungal–bacterial dynamics and their contribution to terrigenous carbon turnover in relation to organic matter quality. *ISME J* 11:415–425. <https://doi.org/10.1038/ismej.2016.131>

- Fanin N, Bertrand I (2016) Aboveground litter quality is a better predictor than belowground microbial communities when estimating carbon mineralization along a land-use gradient. *Soil Biol Biochem* 94:48–60. <https://doi.org/10.1016/j.soilbio.2015.11.007>
- Friedlingstein P, O'Sullivan M, Jones MW et al (2020) Global carbon budget 2020. *Earth Syst Sci Data* 12:3269–3340. <https://doi.org/10.5194/essd-12-3269-2020>
- García-Pausas J, Casals P, Camarero L, Huguet C, Thompson R, Sebastià MT, Romanyà J (2008) Factors regulating carbon mineralization in the surface and subsurface soils of Pyrenean mountain grasslands. *Soil Biol Biochem* 40:2803–2810. <https://doi.org/10.1016/j.soilbio.2008.08.001>
- Guan SY (1986) *Soil enzymology and research method*. Agricultural Press, Beijing
- Guo J, Wang B, Wang G, Wu Y, Cao F (2018a) Vertical and seasonal variations of soil carbon pools in ginkgo agroforestry systems in eastern China. *Catena* 171:450–459. <https://doi.org/10.1016/j.catena.2018.07.032>
- Guo J, Wang G, Geng Q, Wu Y, Cao F (2018b) Decomposition of tree leaf litter and crop residues from ginkgo agroforestry systems in Eastern China: an in situ study. *J Soils Sediments* 18:1424–1431. <https://doi.org/10.1007/s11368-017-1870-6>
- Guo J, Wu Y, Wu X, Ren Z, Wang G (2021) Soil bacterial community composition and diversity response to land conversion is depth-dependent. *Glob Ecol Conserv* 32:e01923. <https://doi.org/10.1016/j.gecco.2021.e01923>
- Hontoria C, Gómez-Paccard C, Mariscal-Sancho I, Benito M, Pérez J, Espejo R (2016) Aggregate size distribution and associated organic C and N under different tillage systems and Ca-amendment in a degraded Ultisol. *Soil Tillage Res* 160:42–52. <https://doi.org/10.1016/j.still.2016.01.003>
- Hu Y, Zheng Q, Noll L, Zhang S, Wanek W (2020) Direct measurement of the in situ decomposition of microbial-derived soil organic matter. *Soil Biol Biochem* 141:107660. <https://doi.org/10.1016/j.soilbio.2019.107660>
- Huang W, Hall SJ (2017) Elevated moisture stimulates carbon loss from mineral soils by releasing protected organic matter. *Nat Commun* 8:1774. <https://doi.org/10.1038/s41467-017-01998-z>
- Huang L, Liu J, Shao Q, Xu X (2012) Carbon sequestration by forestation across China: past, present, and future. *Renew Sustain Energy Rev* 16:1291–1299. <https://doi.org/10.1016/j.rser.2011.10.004>
- Huang J, Lin TC, Xiong D, Yang Z, Liu X, Chen G, Xie J, Li Y, Yang Y (2019) Organic carbon mineralization in soils of a natural forest and a forest plantation of southeastern China. *Geoderma* 344:119–126. <https://doi.org/10.1016/j.geoderma.2019.03.012>
- IPCC (2018) Global warming of 1.5 °C: an IPCC special report on the impacts of global warming of 1.5 °C above pre-industrial levels and related global greenhouse gas emission pathways, in the context of strengthening the global response to the threat of climate change, sustainable development, and efforts to eradicate poverty. Intergovernmental Panel on Climate Change, Geneva, Switzerland
- IUSS Working Group WRB (2015) World reference base for soil resources 2014, Update 2015. International soil classification system for naming soils and creating legends for soil maps. World Soil Resources Report No.106. FAO. <https://www.fao.org/3/i3794en/i3794en.pdf>
- Jeewani PH, Van Zwieten L, Zhu Z, Ge T, Guggenberger G, Luo Y, Xu J (2021) Abiotic and biotic regulation on carbon mineralization and stabilization in paddy soils along iron oxide gradients. *Soil Biol Biochem* 160:108312. <https://doi.org/10.1016/j.soilbio.2021.108312>
- Jin Z, Ping L, Wong M (2020) Systematic relationship between soil properties and organic carbon mineralization based on structural equation modeling analysis. *J Clean Prod* 277:123338. <https://doi.org/10.1016/j.jclepro.2020.123338>
- Kuzyakov Y, Xu X (2013) Competition between roots and microorganisms for nitrogen: mechanisms and ecological relevance. *New Phytol* 198:656–669. <https://doi.org/10.1111/nph.12235>
- Letcher TM (2019) Why do we have global warming? In: Letcher TM (ed) *Managing global warming*. Academic Press, New York, pp 3–15
- Li ZP, Han CW, Han FX (2010) Organic C and N mineralization as affected by dissolved organic matter in paddy soils of subtropical China. *Geoderma* 157:206–213. <https://doi.org/10.1016/j.geoderma.2010.04.015>
- Li WQ, Wu ZJ, Zong YY, Wang GG, Chen FS, Liu YQ, Li JJ, Fang XM (2022a) Tree species mixing enhances rhizosphere soil organic carbon mineralization of conifers in subtropical plantations. *For Ecol Manag* 516:120238. <https://doi.org/10.1016/j.foreco.2022.120238>
- Li Y, Wang T, Camps-Arbestain M, Whitby CP (2022b) The regulators of soil organic carbon mineralization upon lime and/or phosphate addition vary with depth. *Sci Total Environ* 828:154378. <https://doi.org/10.1016/j.scitotenv.2022.154378>
- Liang Z, Elsgaard L, Nicolaisen MH, Lyhne-Kjærbye A, Olesen JE (2018) Carbon mineralization and microbial activity in agricultural topsoil and subsoil as regulated by root nitrogen and recalcitrant carbon concentrations. *Plant Soil* 433:65–82. <https://doi.org/10.1016/j.plantsoil.2018.08.026>
- Liu Z, Zhu M, Wang J et al (2019) The responses of soil organic carbon mineralization and microbial communities to fresh and aged biochar soil amendments. *GCB Bioenergy* 11:1408–1420. <https://doi.org/10.1111/gcbb.12644>
- Lu X, Li Y, Wang H, Singh BP, Hu S, Luo Y, Li J, Xiao Y, Cai X, Li Y (2020) Responses of soil greenhouse gas emissions to different application rates of biochar in a subtropical Chinese chestnut plantation. *Agric For Meteorol* 271:168–179. <https://doi.org/10.1016/j.agrformet.2019.03.001>
- Luo Z, Feng W, Luo Y, Baldock J, Wang E (2017) Soil organic carbon dynamics jointly controlled by climate, carbon inputs, soil properties and soil carbon fractions. *Glob Change Biol* 23:4430–4439. <https://doi.org/10.1111/gcb.13767>
- Ma C, Chen X, Zhang J, Zhu Y, Kalkhajah YK, Chai R, Ye X, Gao HJ, Chu W, Mao JD, Thompson ML (2019) Linking chemical structure of dissolved organic carbon and microbial community composition with submergence-induced soil organic carbon mineralization. *Sci Total Environ* 692:930–939. <https://doi.org/10.1016/j.scitotenv.2019.07.286>
- Moinet GYK, Millard P (2020) Temperature sensitivity of decomposition: discrepancy between field and laboratory estimates is not due to sieving the soil. *Geoderma* 374:114444. <https://doi.org/10.1016/j.geoderma.2020.114444>
- Montagnini F, Nair PKR (2004) Carbon sequestration: an underexploited environmental benefit of agroforestry systems. *Agrofor Syst* 61–62:281–295. <https://doi.org/10.1023/b:agfo.0000029005.92691.79>
- Munda S, Bhaduri D, Mohanty S, Chatterjee D, Tripathi R, Shahid M, Kumar U, Bhattacharyya P, Kumar A, Adak T, Jangde HK, Nayak AK (2018) Dynamics of soil organic carbon mineralization and C fractions in paddy soil on application of rice husk biochar. *Biomass Bioenergy* 115:1–9. <https://doi.org/10.1016/j.biombioe.2018.04.002>
- Nadal-Romero E, Cammeraat E, Pérez-Cardiel E, Lasanta T (2016) Effects of secondary succession and afforestation practices on soil properties after cropland abandonment in humid Mediterranean mountain areas. *Agric Ecosyst Environ* 228:91–100. <https://doi.org/10.1016/j.agee.2016.05.003>
- Neculman R, Matus F, Godoy R, MdLL M, Rumpel C (2021) Carbon mineralization controls in top- and subsoil horizons of two andisols under temperate old-growth rain forest. *J Soil Sci Plant Nutr* 21:780–790. <https://doi.org/10.1007/s42729-020-00400-0>
- Patel KF, Smith AP, Bond-Lamberty B, Fansler SJ, Tfaily MM, Bramer L, Varga T, Bailey VL (2021) Spatial access and resource limitations control carbon mineralization in soils. *Soil Biol Biochem* 162:108427. <https://doi.org/10.1016/j.soilbio.2021.108427>
- Poeplau C, Don A (2013) Sensitivity of soil organic carbon stocks and fractions to different land-use changes across Europe. *Geoderma* 192:189–201. <https://doi.org/10.1016/j.geoderma.2012.08.003>
- Rahman MM, Bårçena TG, Vesterdal L (2017) Tree species and time since afforestation drive soil C and N mineralization on former cropland. *Geoderma* 305:153–161. <https://doi.org/10.1016/j.geoderma.2017.06.002>
- Rong G, Zhang X, Wu H, Ge N, Yao Y, Wei X (2021) Changes in soil organic carbon and nitrogen mineralization and their temperature sensitivity in response to afforestation across China's Loess Plateau. *Catena* 202:105226. <https://doi.org/10.1016/j.catena.2021.105226>
- Roy T, Biswas AK, Sarkar A, Jha P, Sharma NK, Mishra PK, Patra AK (2022) Impact of varied levels of N, P, and S stoichiometry on C mineralization from three contrasting soils with or without wheat straw amendment: a laboratory study. *J Soil Sci Plant Nutr* 22:501–514. <https://doi.org/10.1007/s42729-021-00664-0>
- Sarkar D, Sinha AK, Mukhopadhyay P, Danish S, Fahad S, Datta R (2021) Carbon mineralization rates and kinetics of surface-applied and incorporated rice and maize residues in entisol andceptisol soil types. *Sustainability* 13:7212. <https://doi.org/10.3390/su13137212>
- Scharlemann JPW, Tanner EVJ, Hiederer R, Kapos V (2014) Global soil carbon: understanding and managing the largest terrestrial carbon pool. *Carbon Manag* 5:81–91. <https://doi.org/10.4155/cmt.13.77>

- Schlüter S, Roussety T, Rohe L, Guliyev V, Blagodatskaya E, Reitz T (2022) Land use impact on carbon mineralization in well aerated soils is mainly explained by variations of particulate organic matter rather than of soil structure. *Soil* 8:253–267. <https://doi.org/10.5194/soil-8-253-2022>
- Schmidt MWI, Torn MS, Abiven S et al (2011) Persistence of soil organic matter as an ecosystem property. *Nature* 478:49–56. <https://doi.org/10.1038/nature10386>
- Smith P, Davis SJ, Creutzig F et al (2016) Biophysical and economic limits to negative CO<sub>2</sub> emissions. *Nat Clim Change* 6:42–50. <https://doi.org/10.1038/nclimate2870>
- Tang Z, Sun X, Luo Z, He N, Sun OJ (2018) Effects of temperature, soil substrate, and microbial community on carbon mineralization across three climatically contrasting forest sites. *Ecol Evol* 8:879–891. <https://doi.org/10.1002/ece3.3708>
- Tardy V, Spor A, Mathieu O et al (2015) Shifts in microbial diversity through land use intensity as drivers of carbon mineralization in soil. *Soil Biol Biochem* 90:204–213. <https://doi.org/10.1016/j.soilbio.2015.08.010>
- Tian Q, Yang X, Wang X, Liao C, Li Q, Wang M, Wu Y, Liu F (2016) Microbial community mediated response of organic carbon mineralization to labile carbon and nitrogen addition in topsoil and subsoil. *Biogeochemistry* 128:125–139. <https://doi.org/10.1007/s10533-016-0198-4>
- Wang Q, Zeng Z, Zhong M (2016) Soil moisture alters the response of soil organic carbon mineralization to litter addition. *Ecosystems* 19:450–460. <https://doi.org/10.1007/s10021-015-9941-2>
- Wang X, Bian Q, Jiang Y, Zhu L, Chen Y, Liang Y, Sun B (2021) Organic amendments drive shifts in microbial community structure and keystone taxa which increase C mineralization across aggregate size classes. *Soil Biol Biochem* 153:108062. <https://doi.org/10.1016/j.soilbio.2020.108062>
- Wang M, Guo X, Zhang S, Xiao L, Mishra U, Yang Y, Zhu B, Wang G, Mao X, Qian T, Jiang T, Shi Z, Luo Z (2022) Global soil profiles indicate depth-dependent soil carbon losses under a warmer climate. *Nat Commun* 13:5514. <https://doi.org/10.1038/s41467-022-33278-w>
- Wang W, Zhang H, Vinay N, Wang D, Mo F, Liao Y, Wen X (2023) Microbial functional genes within soil aggregates drive organic carbon mineralization under contrasting tillage practices. *Land Degrad Dev* 34:3618–3635. <https://doi.org/10.1002/ldr.4708>
- Wei X, Zhu Z, Liu Y, Luo Y, Deng Y, Xu X, Liu S, Richter A, Shibistova O, Guggenberger G, Wu J, Ge T (2020) C:N:P stoichiometry regulates soil organic carbon mineralization and concomitant shifts in microbial community composition in paddy soil. *Biol Fertil Soils* 56:1093–1107. <https://doi.org/10.1007/s00374-020-01468-7>
- Wu D, Ren C, Ren D, Tian Y, Li Y, Wu C, Li Q (2023) New insights into carbon mineralization in tropical paddy soil under land use conversion: coupled roles of soil microbial community, metabolism, and dissolved organic matter chemodiversity. *Geoderma* 432:116393. <https://doi.org/10.1016/j.geoderma.2023.116393>
- Xiao H, Li Z, Chang X, Huang J, Nie X, Liu C, Liu L, Wang D, Dong Y, Jiang J (2017) Soil erosion-related dynamics of soil bacterial communities and microbial respiration. *Appl Soil Ecol* 119:205–213. <https://doi.org/10.1016/j.apsoil.2017.06.018>
- Yang S, Jansen B, Absalah S, Kalbitz K, Castro FOC, Cammeraat ELH (2022) Soil organic carbon content and mineralization controlled by the composition, origin and molecular diversity of organic matter: a study in tropical alpine grasslands. *Soil Tillage Res* 215:105203. <https://doi.org/10.1016/j.still.2021.105203>
- You Y, Wang J, Huang X, Tang Z, Liu S, Sun OJ (2014) Relating microbial community structure to functioning in forest soil organic carbon transformation and turnover. *Ecol Evol* 4:633–647. <https://doi.org/10.1002/ece3.969>
- You Y, Wang J, Sun XL, Tang ZX, Zhou ZY, Sun OJ (2016) Differential controls on soil carbon density and mineralization among contrasting forest types in a temperate forest ecosystem. *Sci Rep* 6:22411. <https://doi.org/10.1038/srep22411>
- Zhang S, Fang Y, Luo Y et al (2021a) Linking soil carbon availability, microbial community composition and enzyme activities to organic carbon mineralization of a bamboo forest soil amended with pyrogenic and fresh organic matter. *Sci Total Environ* 801:149717. <https://doi.org/10.1016/j.scitotenv.2021.149717>
- Zhang Y, Ge N, Liao X, Wang Z, Wei X, Jia X (2021b) Long-term afforestation accelerated soil organic carbon accumulation but decreased its mineralization loss and temperature sensitivity in the bulk soils and aggregates. *Catena* 204:105405. <https://doi.org/10.1016/j.catena.2021.105405>
- Zhou Z, Jiang L, Du E, Hu H, Li Y, Chen D, Fang J (2013) Temperature and substrate availability regulate soil respiration in the tropical mountain rainforests, Hainan Island, China. *J Plant Ecol* 6:325–334. <https://doi.org/10.1093/jpe/rtt034>

## Publisher's Note

Springer Nature remains neutral with regard to jurisdictional claims in published maps and institutional affiliations.

Submit your manuscript to a SpringerOpen<sup>®</sup> journal and benefit from:

- Convenient online submission
- Rigorous peer review
- Open access: articles freely available online
- High visibility within the field
- Retaining the copyright to your article

Submit your next manuscript at ► [springeropen.com](https://www.springeropen.com)